Acupuncture and Herbal Medicine

Protective effect of *Camellia nitidissima* Chi on γ rays radiation-induced hematopoietic and gastrointestinal damage

Zhiyun Wang[1,2], Haihua Shang[1], Wenfeng Gou[1], Feifei Xu[1], Yue Hou[1], Gaiting Liu[2], Zhonghao Ren[3], Yiliang Li[1], Yuhua Tian[2], Wei Li[4,*], Yuefei Wang[2,*], Wenbin Hou[1,*]

[1]Institute of Radiation Medicine, Peking Union Medical College & Chinese Academy of Medical Sciences, Tianjin, China; [2]National Key Laboratory of Chinese Medicine Modernization, State Key Laboratory of Component-based Chinese Medicine, Tianjin University of Traditional Chinese Medicine, Tianjin, China; [3]Shenyang Pharmaceutical University, Shenyang, China; [4]Faculty of Pharmaceutical Sciences, Toho University, Funabashi, Chiba, Japan

Abstract

Objective: *Camellia nitidissima* Chi, a Chinese medicine commonly used by ethnic minorities in Guangxi, China, is beneficial for clearing heat, detoxifying, inducing diuresis, and suppressing swelling. It has various pharmacological properties, including antitumor, anti-inflammatory, and antioxidant. However, its potential application in radioprotection remains unclear. In this study, we aimed to determine whether *Camellia nitidissima* Chi has radioprotective effects against radiation-induced gastrointestinal and hematopoietic damage.

Methods: The 1,1-diphenyl-2-picrylhydrazyl (DPPH) free radical and 2,2'-azino-bis(3-ethylbenzothiazoline-6-sulfonic acid) (ABTS) techniques were used to assess the ability of *Camellia nitidissima* Chi to scavenge free radicals. We conducted a 30-day survival rate experiment to evaluate the radioprotective capabilities of *Camellia nitidissima* Chi. Additionally, we developed models of radiation-induced intestinal and hematopoietic damage. Alterations in the white blood cell (WBC) count, total superoxide dismutase (T-SOD), glutathione (GSH), and protein expression linked to apoptosis were observed.

Results: *Camellia nitidissima* Chi scavenged 84.72% and 93.47% of DPPH and ABTS, had a certain radiation protection potential, and increased the survival rate of mice to over 90%. Moreover, following exposure, *Camellia nitidissima* Chi enhanced WBC, T-SOD, and GSH levels. *Camellia nitidissima* Chi increased B-cell lymphoma-extra large (BCL-XL) expression and suppressed Bcl-2 associated X protein (BAX) expression, providing radioprotection to cells.

Conclusions: *Camellia nitidissima* Chi has a strong antioxidant ability; it can improve the survival rate of mice after lethal dose irradiation and protect against radiation-induced hematopoietic and gastrointestinal damage. These findings can serve as a guide for using Chinese medicines for radioprotection.

Keywords: Antioxidant capacity, *Camellia nitidissima* Chi, Gastrointestinal system, Hematopoietic system, Radioprotection

Introduction

Exposure of organisms to ionizing radiation often leads to acute radiation syndrome (ARS)[1,2]. When the entire body or a portion of it is exposed to high radiation doses in a brief amount of time, the organism's water molecules are impacted, and various free radicals, or ROS, are ionized. This leads to oxidative stress and other reactions that cause damage to the organism[3,4]. Ionizing radiation can also act on other substances in the body, causing apoptosis and subsequently affecting homeostasis[5]. Total body irradiation (TBI) and total abdominal irradiation (TAI) can lead to ARS, including hematopoietic, gastrointestinal, and cerebrovascular diseases.

Many drugs have been reported to reduce radiation-induced hematopoietic damage[6] as well as damage to the gastrointestinal tract and other systems, including amphotericin[7], melatonin[8], and N-acetylcysteine[9]. These drugs seriously interfere with optimal treatment due to their numerous side effects (vomiting, nausea, and hypotension), rapid clearance, and off-target effects[10]. Therefore, the search for novel radioprotective agents has become urgent.

Zhiyun Wang and Haihua Shang contributed equally to this work and share first authorship.

**Corresponding author. Wei Li, E-mail: liwei@phar.toho-u.ac.jp; Yuefei Wang, E-mail: wangyf0622@tjutcm.edu.cn; Wenbin Hou, E-mail: houwenbin@irm-cams.ac.cn.*

Received 3 November 2023 / Accepted 13 May 2024

How to cite this article: *Wang ZY, Shang HH, Gou WF, Xu FF, Hou Y, Liu GT, Ren ZH, Li YL, Tian YH, Li W, Wang YF, Hou WB. Protective effect of Camellia nitidissima Chi on γ rays radiation-induced hematopoietic and gastrointestinal damage. Acupunct Herb Med 2024;4(4):487–499. DOI: 10.1097/HM9.0000000000000127*

Global attention to natural medicines has had a growing impact on pharmaceutical research and development. According to the World Health Organization (WHO), up to 80% of the population in many developing countries depend on natural medicines for treatment and recovery, which account for a significant portion of the pharmaceutical market in developed countries[11]. Chinese medicine is an important branch of natural medicine involving holistic treatment. In the development of modern Chinese medicine, various plants, such as *Scutellaria baicalensis*[12], *Andrographis paniculata*[13], *Coix seed*[14], and *Green tea*[15], have demonstrated various protective effects on radiation-induced multi-organ damage; moreover, these medicines are popular because of their nontoxic and broad-spectrum effects. *Camellia nitidissima* Chi (CNC), which is mainly distributed in the southern Guangxi Province, China[16], is known as the "panda of the plant world" and as a "longevity tea," exerting multiple effects such as liver protection[17], antitumor[18,19], and antioxidant activities[20]. It is widely used for treating hyperlipidemia[21], infectious diseases[22], cancer[19,23], and other diseases.

In this study, we first examined the antioxidant capacity of CNC using both the 1,1-Diphenyl-2-picrylhydrazyl (DPPH) and 2,2'-azino-bis(3-ethylbenzothiazoline-6-sulfonic acid) (ABTS) methods, monitored the effect of CNC administration on the survival rate of mice after lethal dose irradiation, evaluated the protective effects of CNC on the hematopoietic system damaged by systemic irradiation and the gastrointestinal system damaged by local irradiation, and conducted a preliminary exploration of its potential mechanism of action. In conclusion, CNC can be developed as a herbal protective agent for radiation protection.

Materials and methods

Chemicals and reagents

DPPH free radical (DPPH) was purchased from TCI (Shanghai, China), ABTS was purchased from Beyotime Biotechnology (Shanghai, China), and Trolox (a vitamin E analog) was purchased from Aladdin (Shanghai, China). The BCL-2 inhibitor, navitoclax, was purchased from MCE (NJ, USA). Dulbecco's modified Eagle's medium (DMEM) and Dulbecco's modified Eagle's medium/nutrient mixture *F*-12 (DMEM/F12) were purchased from Thermo Fisher Scientific (Waltham, MA, USA). Fetal bovine serum (FBS) was obtained from Biological Industries (Panama, Israel) and penicillin-streptomycin was obtained from Beyotime Biotechnology.

Plant materials and extract preparation

CNC was purchased from Fangchenggang, Guangxi, China; it was harvested in September 2020, dried, ground, sieved through a 40-sieve, sealed, and stored at room temperature under dry conditions.

Water extracts were prepared using the decoction method. Briefly, 50 g of CNC was mixed with 1,000 mL of deionized water at a ratio of 1:20 (mass:volume), heated to 100°C, boiled, and then filtered after 1 hour of decoction. Then, 1,000 mL of deionized water was added to the filter residue, heated again to 100°C, boiled for 1 hour, and then cooled naturally to obtain the secondary filtrate. The two filtrates were combined and stored in a sealed container at low temperature [Supplementary Figure 1, http://links.lww.com/AHM/A131].

DPPH assay

We used a total of 20 μL of different CNC concentrations and added 180 μL of DPPH solution (200 μmol/L). After 30 minutes of incubation at 25°C in the dark, the absorbance at 517 nm was measured, and the DPPH radical scavenging rate of CNC was calculated.

The inhibition of DPPH = $[(A_{blank} - A_{CNC})/A_{blank}] \times 100\%$, A_{CNC} is the absorbance of the tested sample, and A_{blank} is the absorbance of the blank (a solvent mixture instead of the sample solution was mixed with the DPPH radical solution).

ABTS assay

As per the manufacturer's instructions, the ABTS working solution was preconfigured for 12 to 16 hours in time and diluted 50 times during use. Then, 10 μL CNC with different concentrations was prepared, and 200 μL ABTS working solution was added. After incubation in the dark for 5 minutes, absorbance was measured at 405 nm.

The inhibition of ABTS = $[(A_{blank} - A_{CNC})/A_{blank}] \times 100\%$, A_{CNC} is the absorbance of the tested sample and A_{blank} is the absorbance of the blank (a solvent mixture instead of the sample solution was mixed with the ABTS radical solution).

Animals

Specific pathogen-free (SPF) male C57BL/6 mice [6–8 weeks old, (18 ± 2) g] were obtained from HFK Bioscience (Beijing, China) and maintained under SPF conditions at the Animal Facility of Radiation Medicine, Chinese Academy of Medical Sciences (IRM). All the mice were housed at a relative humidity of 40% to 60%, a housing temperature of 18°C to 25°C, and under a 12-hour dark/light cycle. This study was reviewed and approved by the Animal Ethics Committee of the Institute of Radiation Medicine, Chinese Academy of Medical Sciences, under the ethics number: IRM-DWLL-20211218, IRM-DWLL-20211219, IRM-DWLL-20211220.

Groups and administration

For the survival experiment, 40 mice were randomly divided into four groups: radiation and radiation + CNC (0.4, 0.8, and 1.2 g/kg), administered by gavage once daily for 5 days before and 7 days after irradiation.

For the experiment on radiation damage to the hematopoietic system, 50 mice were randomly divided into five groups: control, radiation, and radiation + CNC (0.4, 0.8, 1.2 g/kg) by gavage administration for 5 days before and 7 days after radiation.

For the radiation-induced intestinal injury experiment, 50 mice were randomly divided into five groups: control, radiation, and radiation + CNC (0.4, 0.8, and 1.2 g/kg).

Radiation

A Gammacell® 40 Exactor ^{137}Cs γ-ray source (Best Theratronics, Canada) was used for irradiation at doses of 7.2, 4, and 13 Gy at a dose rate of 0.99 Gy/min.

The survival rate experiment (7.2 Gy) and hematopoietic system damage experiment (4 Gy) involved whole-body irradiation, whereas the radiation-induced intestinal damage experiment (13 Gy) used a partial irradiation method[24–27].

30-Day survival assay

Daily survival data were collected from the experimental mice in each group following 7.2 Gy of irradiation. All surviving mice were sacrificed using isoflurane overdose anesthesia on the 30th day after irradiation, and the survival rate and survival time of the mice were analyzed.

Hematological parameter measurement

On the seventh day after 4 Gy TBI, blood samples were collected from the mice under isoflurane respiratory anesthesia in anticoagulation tubes containing ethylenediaminetetraacetic acid dipotassium (EDTA-K2) using the enucleation method. Red blood cell (RBC), white blood cell (WBC), platelet (PLT), hemoglobin (HGB), and lymphocyte (lymph) counts were determined using a hematological analyzer (BC-2800vet Fully Automated Hematology Analyzer, Shenzhen, China).

Analysis of bone marrow nucleated cells from the femur

The unilateral femurs of the mice were removed, and 1 mL of pre-chilled PBS was withdrawn using a sterile syringe and gently injected into the bone marrow cavity of the femur. The bone marrow cells (soft red tissue within the bone) were slowly flushed out and collected until all the red bone marrow was removed and the bone turned white. The collected bone marrow cell suspension was placed on ice, shaken, filtered through a 200-mesh sieve, and analyzed using a hematological analyzer to determine the number of nucleated cells.

Organ index assay

After the experiment, we removed and weighed the spleen, thymus, gonads, pancreas, lungs, and kidneys of each group of mice.

Total superoxide dismutase (T-SOD) and glutathione (GSH) assay

The fresh livers of the mice in each group were harvested and mechanically homogenized by adding pre-cooled normal saline to produce a 10% homogenate in an ice water bath at 7 days after irradiation. The homogenate was centrifuged at 3,000 rpm/min for 10 min, and the supernatant was removed.

The BCA method (Shanghai, China) was used to determine the protein concentration in the liver tissue, and total superoxide dismutase (T-SOD) activity and GSH content were determined per the manufacturer's instructions (Nanjing Jiancheng Bioengineering Institute, Nanjing, China).

Hematoxylin and eosin (H&E) staining

At 3.5 days post-irradiation, the mice were eviscerated, and the colon was collected and fixed in a 10% neutral buffered formalin solution, embedded in paraffin, and sectioned transversely to a thickness of 5 μm, then stained with H&E to observe the intestinal histological changes in the mice.

Colon length

On the 3.5th day after irradiation, when the samples were taken from the mice in each group, the abdomens of the mice were opened, and the cecum was cut off from the cecum of the mice to the anus of the mice and placed in utensils. Their lengths were then measured and photographed for preservation.

Diarrhea score

After local irradiation with 13 Gy, the fecal status of each group of mice was detected every day and scored (Table 1): 0 was a normal stool, 1 indicated that the feces had lost their existing shape, 2 indicated significant dysentery and significant filth near the anus, 3 indicated the presence of bloody stools or severe dysentery, as well as large amounts of muck in the tail and anus[28,29].

RT-qPCR

Total RNA was extracted from 40 mg of colon samples using TRIzol reagent (CW0580, CWBIO). RNA concentration was measured using an ultra-micro UV spectrophotometer. Next, genomic DNA was removed, and the RNA was reverse transcribed using a HiFiScript gDNA Removal cDNA Synthesis Kit (CW2582M, CWBIO) per the manufacturer's instructions. Next, 2 μL of the prepared cDNA was used for detection using real-time quantitative fluorescence PCR (ABI 7500 real-time fluorescence quantitative PCR instrument; Applied Biosystems, USA). β-Actin was selected as the internal reference gene. The primers used in this experiment were synthesized by Sangon Biotech [Supplementary Data, http://links.lww.com/

Table 1

Diarrhea status and scoring criteria in mice

State of feces	Score
Normal shape	0
Lost original shape	1
Apparent dysentery with anal fouling	2
Severe dysentery with bloody stools	3

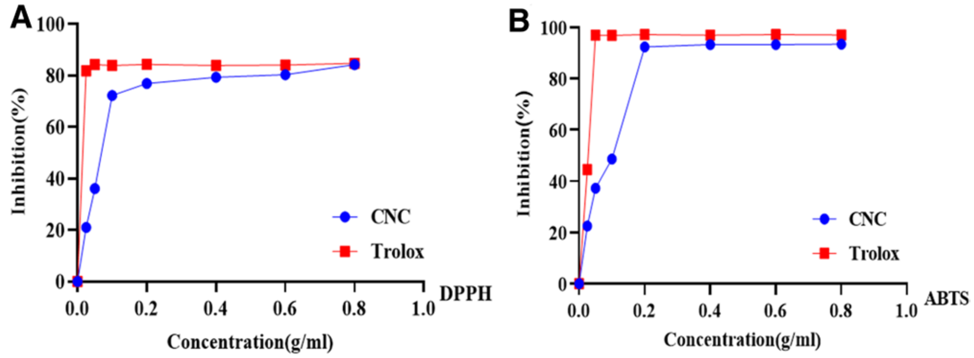

Figure 1. Detection of the *in vitro* antioxidant capacity of CNC at different concentrations. (A) DPPH assay was used to detect the antioxidant capacity of CNC. (B) The antioxidant capacity of the CNC was determined using the ABTS method. $n \geq 3$ in each group. ABTS: 2,2'-Azino-bis(3-ethylbenzothiazoline-6-sulfonic acid); CNC: *Camellia nitidissima* Chi; DPPH, 1,1-Diphenyl-2-picrylhydrazyl.

AHM/A132]. Real-time quantitative PCR results were analyzed using the $2^{-\Delta\Delta Ct}$ method, and mRNA expression levels were expressed as fold change relative to the mean of the control group.

Cell culture

Human normal intestinal epithelial cell line HIEC-6 and human colon cancer cells HT29 were purchased from Zhongqiaoxinzhou Biotechnology (Shanghai, China) and cultured in DMEM or DMEM/F12 medium supplemented with 10% FBS and 1% penicillin/streptomycin, at 37°C, with 5% CO_2.

Cell viability assay

Cells in the logarithmic growth phase were inoculated into 96-well plates at a density of 3,000 cells/well; and different CNC concentrations were added and incubated for 24, 48, and 72 h, followed by methylthiazolyldiphenyl-tetrazolium bromide (MTT) addition (ST316; Shanghai, China). After incubation for 4 h, the absorbance was measured at 570 nm using an ELISA reader (Tecan, Switzerland) to compare the effects of different CNC concentrations on cell viability.

Clone formation experiments

Cells in the logarithmic growth phase were inoculated into 24-well plates at a density of 50 cells/well and incubated at 37°C for 24 h. CNC was added (30 or 300 μg/mL), and after 2 h, the cells were irradiated at 2, 4, 6, and 8 Gy. Thereafter, 14 days after irradiation, colonies were stained with crystal violet solution and counted.

Western blot analysis

Total protein extracts were subjected to sodium dodecyl sulphate-polyacrylamide gel electrophoresis (SDS-PAGE) and then transferred to a polyvinylidene fluoride (PVDF) membrane. Membranes were blocked with 5% skim milk powder for 2 h. The antibodies were diluted and incubated overnight at 4°C. After washing with PBST, the membranes were incubated with horseradish peroxidase (HRP)-conjugated anti-goat, anti-mouse, or anti-rabbit secondary antibodies and then imaged using a multifunctional molecular imaging system (Alliance MINI HD9, USA) by enhanced chemiluminescence (Beyotime Biotechnology).

The antibodies used in the experiments were purchased from Proteintech (Wuhan, Hubei Province, China) and included poly ADP-ribose polymerase (PARP) (13371-1-AP, 1:1000), Bcl-2 associated X protein (BAX) (13371-1-AP, 1:2,000), B-cell lymphoma-extra large (BCL-XL) (26967-1-AP, 1:1,000), and β-actin (20536-1-AP, 1:1,000).

Statistical analysis

Experimental data were processed and analyzed using the GraphPad Prism 8.0.1 statistical analysis software. Statistical significance of the differences between the means was established using ANOVA. *P* values ≤0.05 were considered statistically significant.

Results

CNC has better free radical scavenging ability

Radiation produces numerous free radicals such as reactive oxygen species, which can disrupt the redox balance of the body and induce a series of pathological conditions[30]. To investigate whether CNC can scavenge free radicals, we used DPPH and ABTS assays[31–32]. The results demonstrated that CNC had a significant anti-oxidation ability for both DPPH and ABTS radicals compared to Trolox (a water-soluble vitamin E analog), a commonly used antioxidant, and there was no significant difference in their antioxidant capacity. The scavenging rate of CNC for DPPH radicals was 86.9% (Figure 1A), and that for ABTS radicals was 93.47% (Figure 1B), indicating significant free radical scavenging ability.

These results confirm that CNC has antioxidant potential *in vitro*; however, their potential for radiation protection remains to be determined.

CNC exerts radioprotection by promoting intestinal epithelial cell proliferation and increasing cell viability

We used an MTT assay to measure the effect of CNC on the viability of HIEC-6 intestinal epithelial cells[33]. The results demonstrated that the CNC had no significant toxic side effects on HIEC-6 cells while increasing cell viability (Figure 2A–C). At the same time, CNC had no radioprotective effect on colon cancer cells HT29 and demonstrated some inhibitory suppressive effect at higher drug concentrations, similar to 1 mg/mL (Figure 2D). This suggests that the drug likely ameliorates the damage caused by radiation. Therefore, we performed a colony formation assay to examine the effect of the drug on the proliferative capacity of irradiated cells[34]. Briefly, cells were treated with CNC at 30 and 300 μg/mL based on the effect of different concentrations on HIEC-6 cell viability in the MTT assay and the consideration that CNC itself is not toxic to cells as a radioprotective agent.

The cells treated with CNC were irradiated at different doses (2, 4, 6, and 8 Gy) and stained with crystal violet. We found that the number of cells in the irradiated group decreased as the radiation dose increased. When the radiation dose reached 8 Gy, the cell survival rate was almost zero (Figure 2E, F). When the radiation dose was 0 Gy, CNC treatment significantly promoted cell proliferation compared to the blank group. When the irradiation dose was increased to 2, 4, 6, and 8 Gy, the CNC treatment groups demonstrated a significant increase in the number of cell colonies compared to the untreated cells. These results indicated that CNC could improve

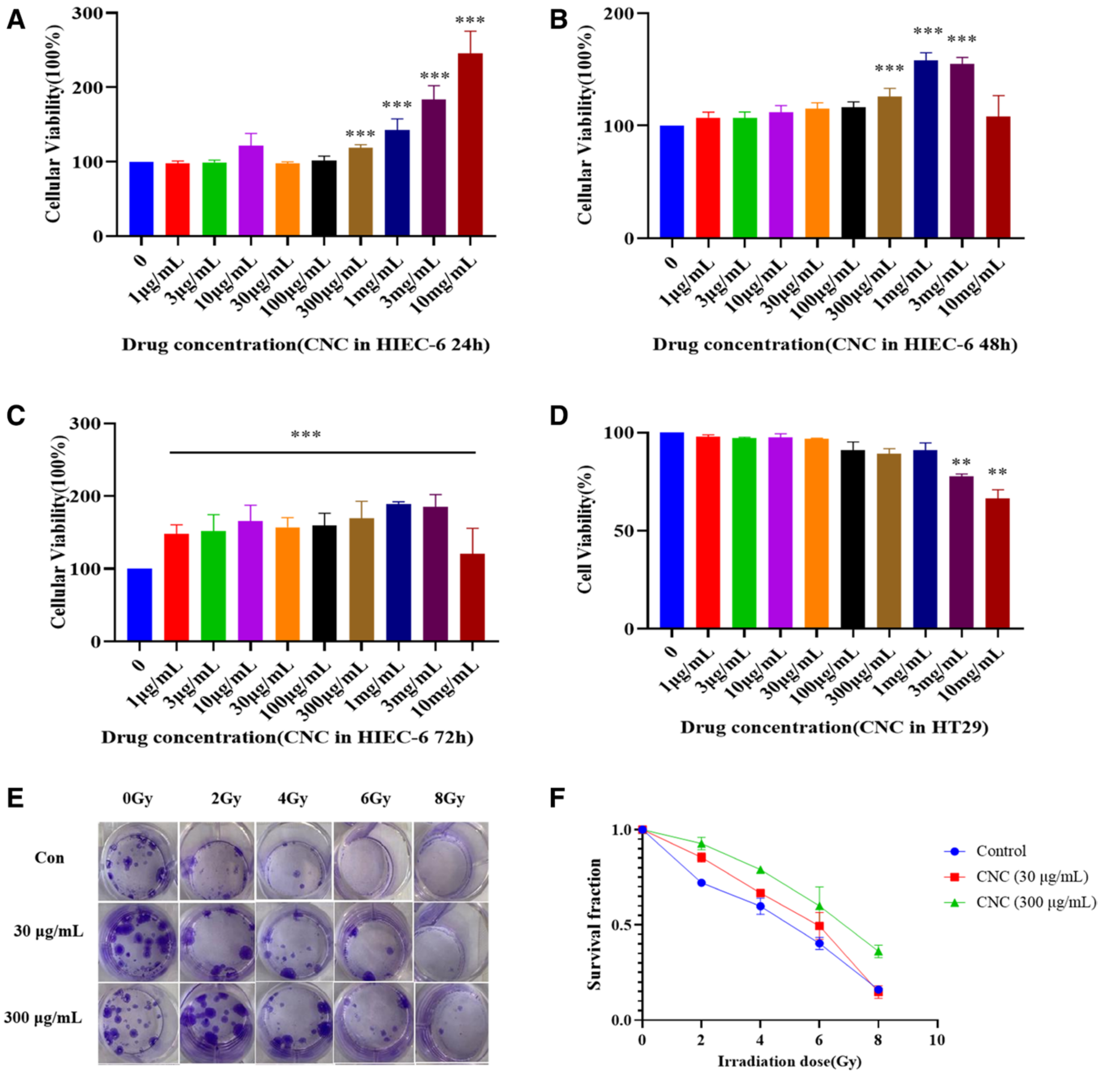

Figure 2. CNC can increase intestinal epithelial cell viability, promote cell proliferation, and reduce radiation damage. Effects of different CNC concentrations on HIEC-6 cell viability at 24 (A), 48 (B), and 72 h (C). (D) The effect of CNC on HT29 cell viability. (E) Cell colony formation after CNC treatment. (F) Cell survival analysis. Data are expressed as the mean ± SD of three independent experiments ($n = 3$). A minimum of three independent experiments were performed. $^{\#}P < 0.05$, compared with the control; $^{***}P < 0.001$, compared with the IR group. CNC: *Camellia nitidissima* Chi; IR: Irradiated; SD: Standard deviation.

the proliferative ability of HIEC-6 cells both with and without irradiation.

CNC improves the survival rate of mice exposed to lethal doses of radiation

Some studies have shown that at radiation doses of 6 to 8 Gy, the body tends to exhibit intense ARS until death[35]. Simultaneously, to confirm whether CNC could scavenge radiation damage, we performed a survival rate experiment at a lethal dose of 7.2 Gy[36] (Figure 3A–C), and found that mice in the irradiated group began dying on the 13th day after irradiation and continued to die over time; however, mice treated with 0.4 g/kg did not die and demonstrated 100% survival throughout the experiment (Figure 3A). The survival rate of the mice with the 0.8 and 1.2 g/kg doses was 90% (Figure 3B, C), which was significantly higher than that in the irradiated group, indicating that CNC can play a protective role and improve the survival rate of mice exposed to lethal doses of radiation.

The median survival times in the irradiated group and all CNC dose groups were 21.5 and 30 days, respectively, further proving the radioprotective effect of CNC on mice (Figure 3D). In summary, CNC can scavenge DPPH and ABTS free radicals with an antioxidant capacity similar to that of Trolox; furthermore, CNC can improve the survival rate of mice subjected to 7.2 Gy whole-body irradiation.

CNC improves the damage to the hematopoietic system caused by 4 Gy TBI

The hematopoietic system is particularly sensitive to radiation, and TBI of 2-6 Gy has been reported to damage the hematopoietic system[35,37]. To verify the radioprotective effect of CNC, we subjected mice to TBI at 4 Gy with or without CNC administration (Figure 4A).

The first changes that occur after exposure to ionizing radiation are hematological[38]. We examined the routine blood indices in each group of mice after TBI with 4 Gy and found that compared to the control group, the RBCs, WBCs, PLTs, HGB levels, and percentage of lymphocytes (lymph) in the peripheral blood of mice in the irradiated group decreased significantly after irradiation (Figure 4B–F). In contrast, all routine blood indices of the CNC-treated mice were significantly better than those of the irradiated group ($P < 0.05$). We examined the number of nucleated cells in the bone marrow (Figure 4G) and found that radiation seriously damaged the hematopoietic function of the mice. However, the number of nucleated cells in the femoral bone marrow of the mice in the CNC administration group was significantly higher than that in the irradiated group. This suggests that CNC alleviates radiation-induced damage to the hematopoietic system.

Similarly, the results of the organ indices demonstrated that the spleen and thymus organ indices in the irradiated group were significantly decreased compared with those in the control group, whereas these were improved to some extent in the CNC group compared with those in the irradiated group. However, there was no significant change in other organ indices compared with those in the irradiated group (Figure 5A–4G).

To verify whether CNC can exert antioxidant capacity *in vivo* and scavenge a large number of free radicals produced by radiation, we first measured T-SOD activity in the livers of mice (Figure 5H). The results demonstrated that the hepatic T-SOD activity of mice in the irradiated group was significantly lower than that

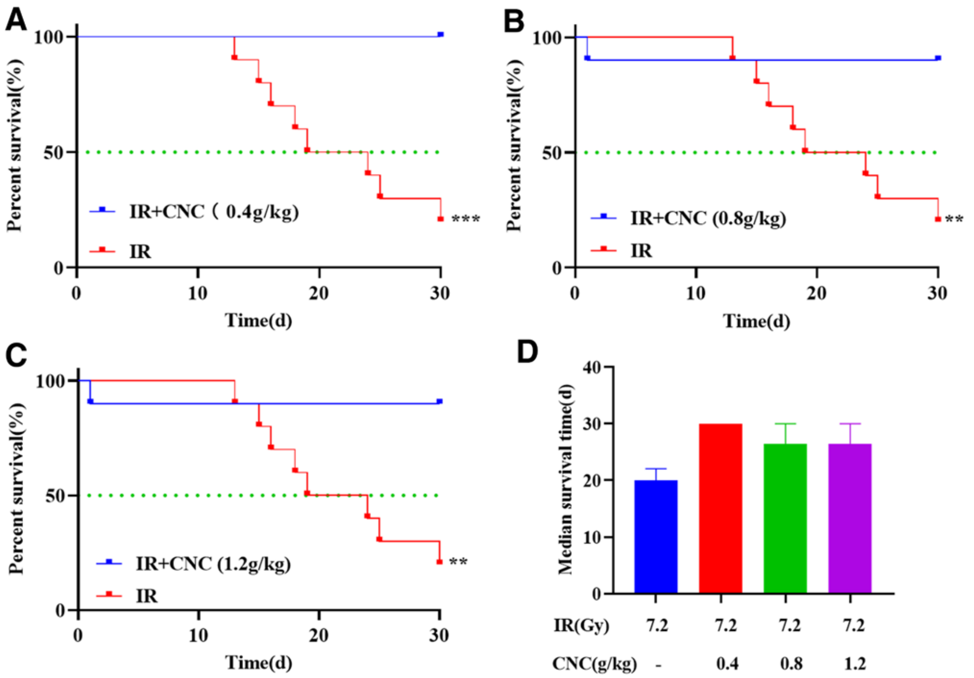

Figure 3. Effect of different CNC concentrations on the 30-day survival of mice exposed to a lethal dose of radiation (7.2 Gy). Differences in survival between the CNC and IR groups at different doses: (A) 0.4 g/kg, (B) 0.8 g/kg, and (C) 1.2 g/kg. (D) Comparison of the median survival times between the CNC and irradiated groups. $n = 10$ mice/group. A minimum of three independent experiments were performed. $^{**}P < 0.01$ compared to the IR group, $^{***}P < 0.001$ compared to the IR group. CNC: *Camellia nitidissima* Chi; IR: Irradiation.

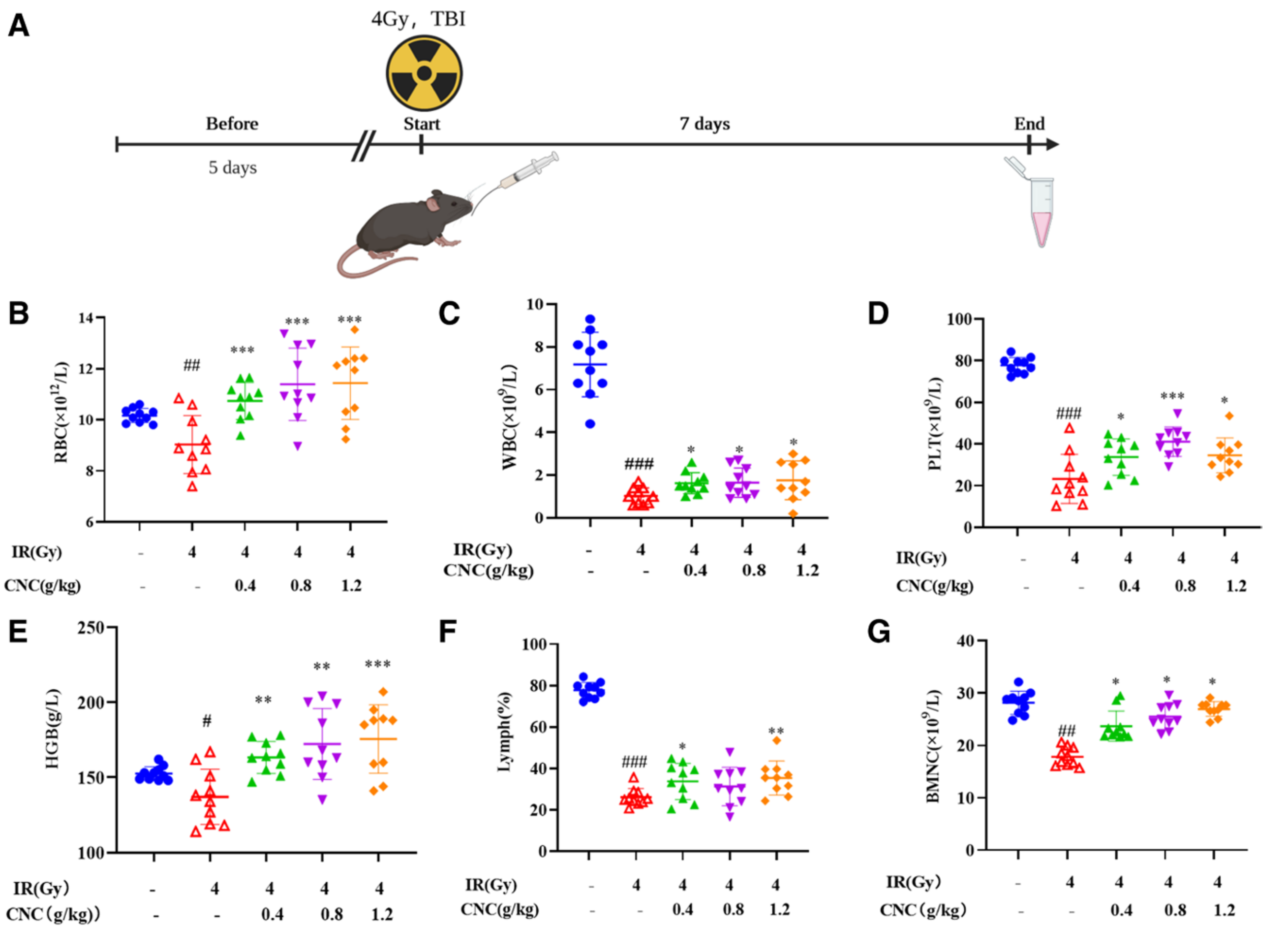

Figure 4. Protective effect of CNC against radiation damage to the hematopoietic system. (A). Duration of CNC administration and IR dose. Changes in peripheral blood cells: (B) RBCs, (C) WBCs, (D) PLT, (E) HGB, and (F) lymph. (G) Number of BMNC in mouse femora. $n = 10$ mice/group. A minimum of three independent experiments were performed. $^{\#}P < 0.05$, $^{\#\#}P < 0.01$, $^{\#\#\#}P < 0.001$ compared to the control; $^{*}P < 0.05$, $^{**}P < 0.01$, $^{***}P < 0.001$ compared to the IR group. BMNC: Bone marrow nucleated cells; CNC: *Camellia nitidissima* Chi; HGB: Hemoglobin; IR: Irradiation; lymph: Lymphocyte percentages; PLT: Platelets; RBCs: Red blood cells; TBI: Total body irradiation; WBC: White blood cells.

in the control group, indicating damage to the antioxidant enzyme activity of the body caused by the large number of free radicals produced by radiation, which disrupted the redox balance[39]. However, compared to the irradiated group, the hepatic T-SOD activity of the CNC group was significantly higher (Figure 4H), indicating that CNC can exert antioxidant activity *in vivo* and scavenge radiation-generated free radicals to a certain extent to decrease the degree of damage to the organism. We also examined GSH content in the liver (Figure 5I). The hepatic GSH content of mice in the irradiated group was significantly higher than that in the control group, indicating that the content of non-enzymatic antioxidants in the livers of mice was also affected by irradiation[39,40]. Compared to the irradiated group, the CNC-administered mice demonstrated significantly higher GSH content in the liver, suggesting that CNC can exert antioxidant capacity *in vivo* and reduce radiation-induced damage.

CNC reduces radioactive intestinal damage caused by abdominal irradiation

Local irradiation at 8 to 15 Gy has been reported to cause gastrointestinal syndromes[41,42]. Therefore, to determine whether CNC plays a radioprotective role in local irradiation, we used TAI at 13 Gy to generate a model of radiation-induced damage to the gastrointestinal system and evaluated the radioprotective effect of CNC (Figure 6A).

Changes in body weight are often considered direct indicators of the protective effects in irradiated mice. We found that, compared with the control group, the body weight of irradiated mice decreased significantly, whereas the body weight of the CNC (0.4 g/kg) group was preserved with some significance (Figure 6B). Thus, CNC can reduce weight loss caused by irradiation to some extent. Colon length is often used to evaluate the severity of intestinal injury[43]. The colon length of the mice in each group was analyzed 3.5 days after irradiation (Figure 6C, D). The results demonstrated that compared with the control group, the colon length of mice in the irradiated group was significantly decreased; however, the colon length in the CNC-administered group was significantly higher than that in the irradiated group.

High doses of radiation to the abdomen often damage the gastrointestinal system, resulting in diarrhea[44]. Based on the fecal analysis of each group, we found that the control group demonstrated normal feces, whereas the irradiated mice demonstrated obvious blood and a

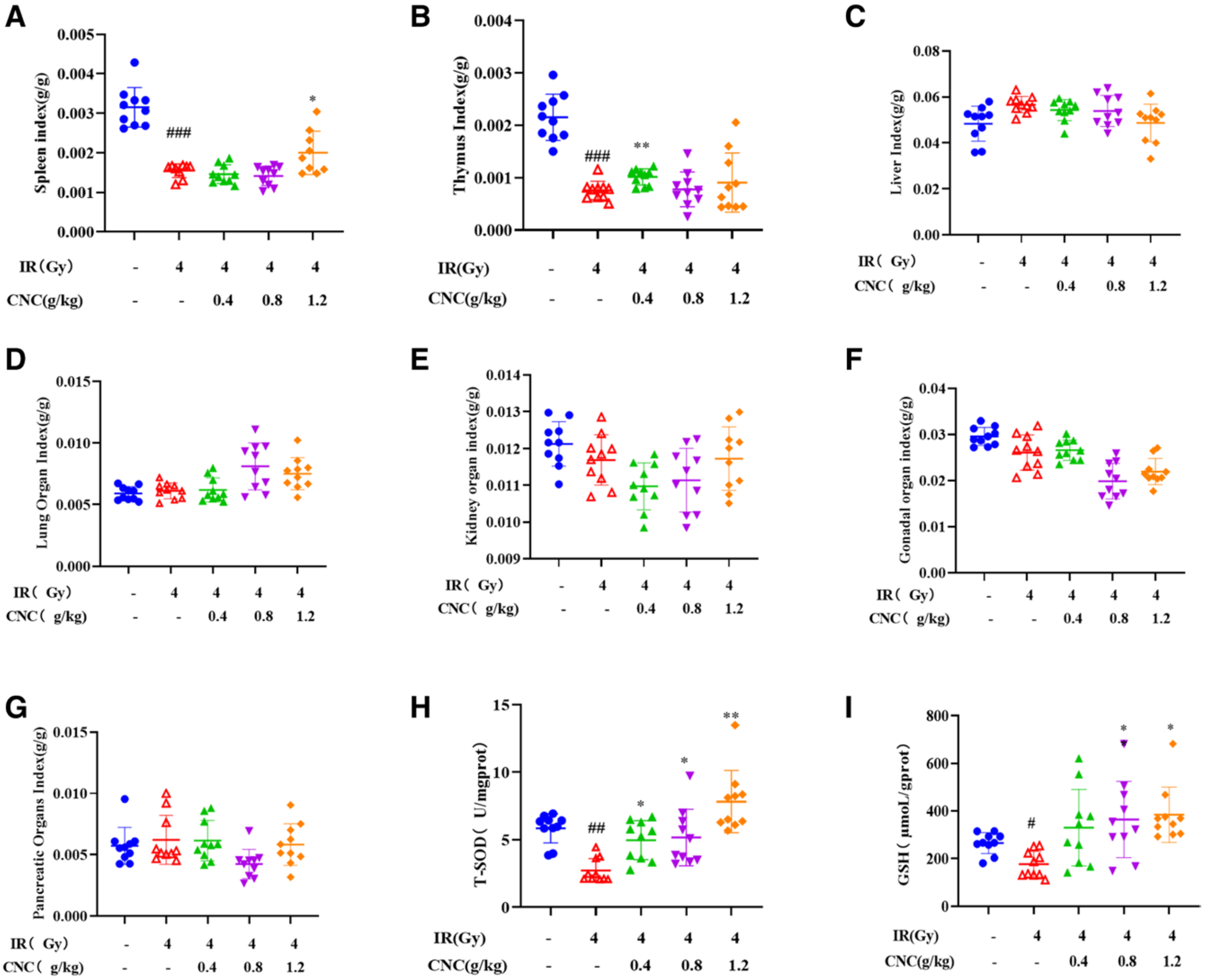

Figure 5. Effect of CNC on organ indices and antioxidants in the body after total body IR at 4 Gy. (A) Spleen indices of mice in control, irradiated, and CNC-administered groups. (B) The thymic index of mice in each group after CNC administration. (C). Changes in liver indices. (D). Lung organ indices by group. (E). Kidney organ index. (F). Gonadal organ index. (G). Pancreatic organ index. Changes in the T-SOD activity (H) and GSH content (I) in the liver of each mouse group. $n = 10$ mice/group. A minimum of three independent experiments were performed. $^{\#}P < 0.05$, $^{\#\#}P < 0.01$, $^{\#\#\#}P < 0.001$ compared to the control, $^{*}P < 0.05$, $^{**}P < 0.01$ compared to the IR group. CNC: *Camellia nitidissima* Chi; GSH: Glutathione; IR: Irradiation; T-SOD: Total superoxide dismutase.

large amount of fecal residue near the anus, indicating severe damage to the intestine accompanied by severe diarrhea after irradiation (Figure 6E).

CNC ameliorates the intestinal villus and crypt injury caused by TAI

To investigate the effect of CNC on radiation-induced intestinal injury, we analyzed the histological changes in the colons of mice. H&E staining results demonstrated that 3.5 days after TAI with 13 Gy, the colons of mice in the irradiated group demonstrated significant changes, such as crypt destruction and shortening of villi, relative to those in the control group. Compared with the irradiated group, the length of the villi in the colon of CNC-administered mice was significantly longer (Figure 7A, B).

Because ionizing radiation can damage intestinal permeability and produce numerous inflammatory factors, thus affecting intestinal epithelial cell proliferation and differentiation, we analyzed the expression of these genes in mouse intestines[12,45]. The experimental results demonstrated that the mRNA expression of Lgr5, Axin2, and ZO-1 in the irradiated group was significantly lower than that in the control group, whereas the interleukin-6 (IL-6) mRNA expression increased significantly, indicating that irradiation caused serious damage to the intestinal permeability. Compared to the irradiated group, the mRNA expression of Lgr5, Axin2, and ZO-1 was significantly higher in the CNC group, whereas the IL-6 expression was lower, indicating that CNC could prevent radiation-induced intestinal damage (Figure 7C–F).

CNC exerts radiation protection by inhibiting radiation-induced cell death

We examined the expression of BAX, BCL-XL, and PARP using western blot analysis in each group of cells 48 h after irradiation. The results demonstrated that the expression of BCL-XL was significantly decreased

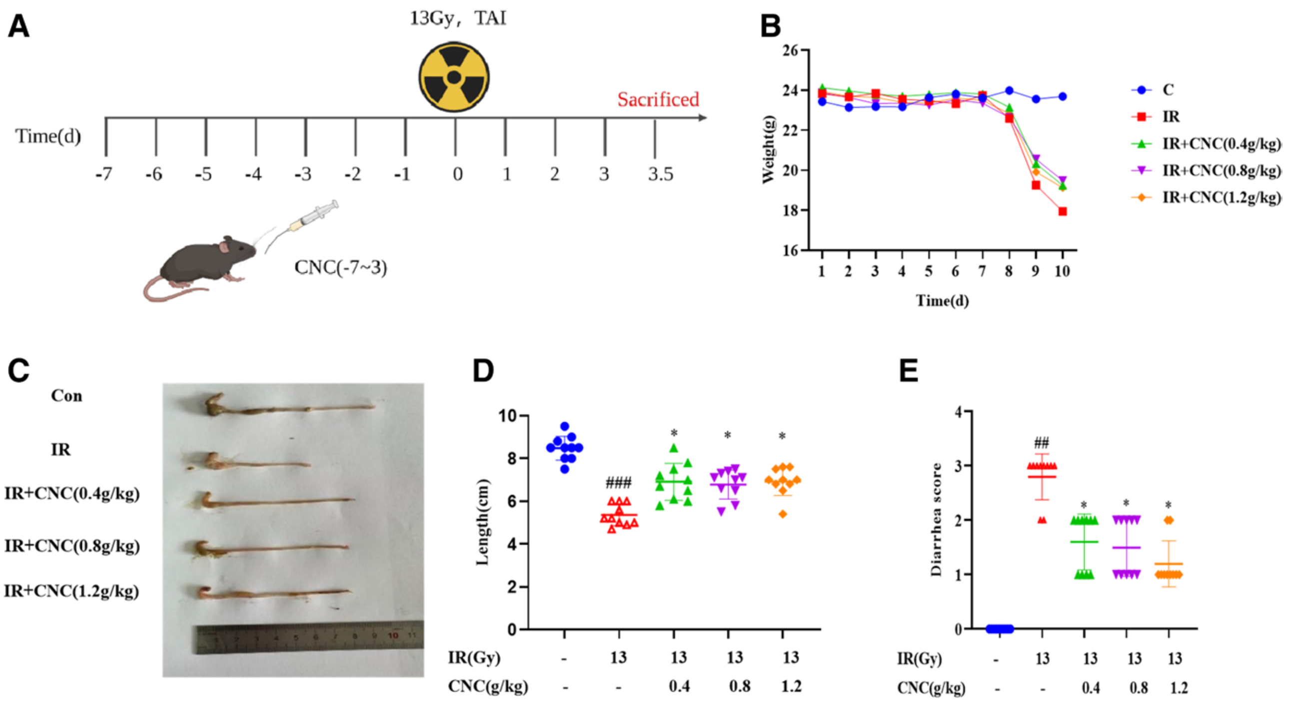

Figure 6. CNC can relieve intestinal damage caused by TAI at 13 Gy. (A) TAI duration and dose. (B) Changes in the body weight of mice in each group after TAI. (C) Comparison of colon lengths after irradiation at 3.5 days. (D). Changes in colon length after irradiation and drug administration. (E). Diarrhea scores of mice in each group after irradiation. $n = 10$ mice/group. A minimum of three independent experiments were performed. $^{\#\#}P < 0.01$, $^{\#\#\#}P < 0.001$ compared to the control, $^{*}P < 0.05$ compared to the IR group. CNC: *Camellia nitidissima* Chi; IR: Irradiated; TAI: Total abdominal irradiation.

after irradiation but increased after drug administration (Figure 8A). We also examined the expression of the apoptosis regulatory proteins BAX and PARP and found that irradiation significantly increased the expression of BAX and PARP compared with that in the control group, whereas the expression of BAX and PARP was significantly decreased in the CNC-administered group when compared with that in the irradiated group (Figure 8B–D). We selected the BCL-2 inhibitor, navitoclax, for validation. The results demonstrated that the expression of BAX was significantly upregulated, and the expression of BCL-XL was inhibited to a certain extent after adding navitoclax, which further proved that CNC could inhibit radiation-induced apoptosis. Furthermore, the colony formation assay demonstrated that the pro-proliferative ability of irradiated cells was significantly inhibited by CNC after adding navitoclax (Figure 8E–G).

Discussion

The hematopoietic[46], gastrointestinal[47], reproductive[48], and central nervous systems[49] are highly sensitive to radiation. Hematopoietic and gastrointestinal systems are important for radioprotective agent development[50,51]. However, drug development is often limited by toxic side effects. Therefore, the search for potential drugs with low or no toxicity has gained increasing importance and is challenging in the field of radiation[52].

To determine the antioxidant capacity of CNC *in vivo*, we performed a 30-day survival experiment in mice subjected to 7.2 Gy irradiation and determined the survival rate difference between the irradiated and CNC-administered groups. The results demonstrated that the irradiated group had a final survival rate of 30%, whereas the survival rates of the CNC-administered mice were significantly higher than those of the irradiated group.

At radiation doses of 1 to 7 Gy, the hematopoietic system is often susceptible to damage, resulting in reduced blood and platelet counts[51]. Therefore, we investigated the ability of CNC to improve hematopoietic system damage after radiation and found that upon whole-body irradiation at 4 Gy, CNC improved the radiation-induced blood indices of blood cells. It can also exert antioxidant effects *in vivo*, as indicated by increased T-SOD activity and GSH content in the liver, thus maintaining a balance between pro-oxidants and antioxidants, reducing ROS-mediated cell damage, and exerting protective effects. These results further confirm the DPPH and ABTS assay results.

At radiation doses ≥8 Gy, the gastrointestinal system exhibits damage and is prone to acute gastrointestinal syndromes, as evidenced by the loss of intestinal crypts, villus shortening, and gastrointestinal mucosal barrier disruption, owing to a combination of oxidative stress, DNA strand breaks, and altered expression of apoptotic signaling proteins[51,53,54]. We irradiated mice with 13 Gy to the abdomen and evaluated the changes after 3.5 days; we found that irradiation destroyed the villi and crypts of the colon and shortened the colon length, which is key to intestinal regeneration, whereas the CNC-administered group demonstrated retention of colon length along with integrity of the epithelial villi and crypts to some extent. Furthermore, the fecal

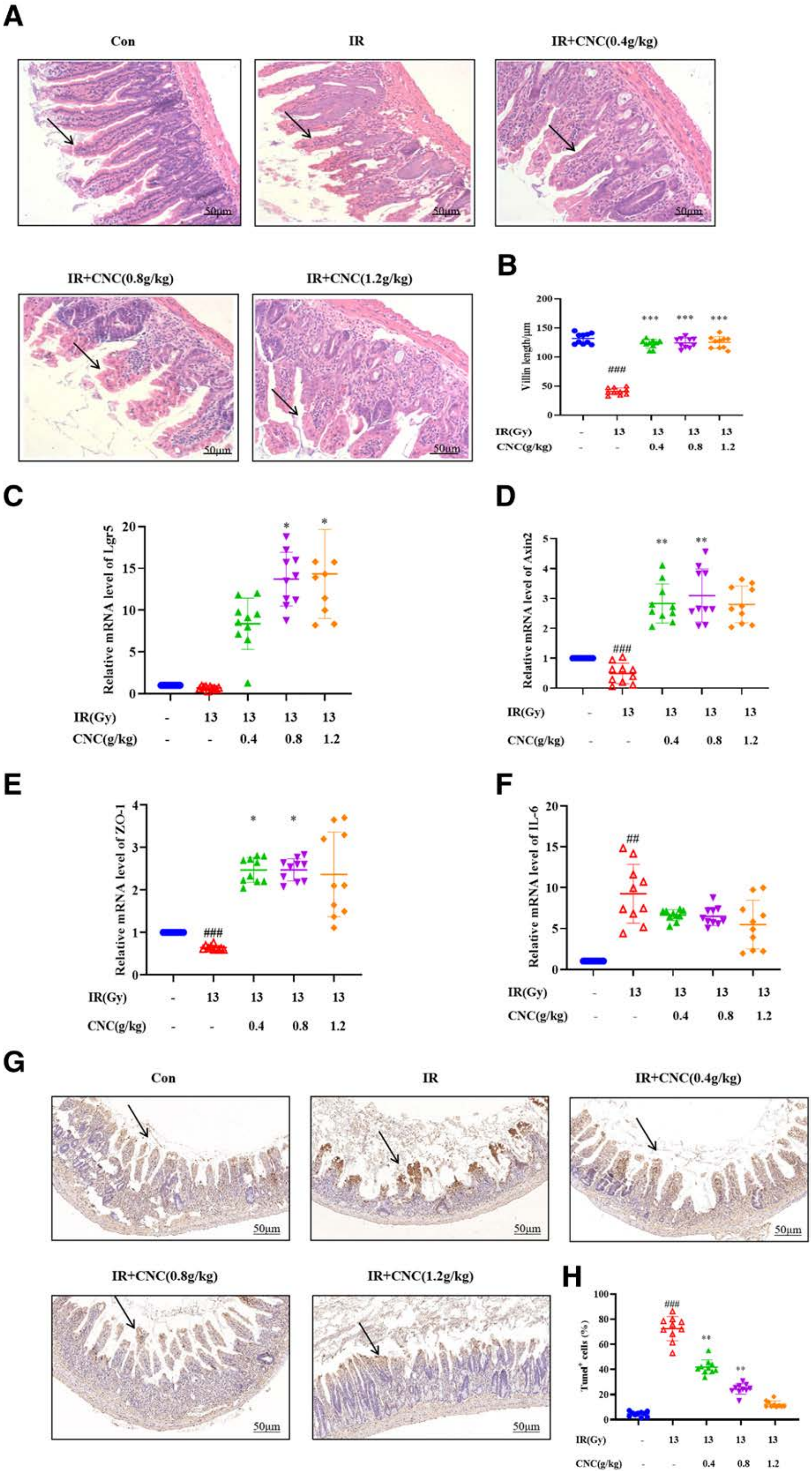

Figure 7. Intestinal protective effect of CNC under 13 Gy TAI. (A) H&E staining of mouse intestinal tissues. The "→" symbols in the figure mark the villi of the small intestine. (B) Villus length in the small intestines of each group. Lgr5 (C) and Axin2 (D) mRNA expression in the intestinal tissues of each group. (E). Effect of CNC on intestinal mucosal barrier permeability after irradiation. (F). Ameliorative effects of CNC on intestinal inflammation after irradiation. (G). TUNEL staining of mouse intestinal tissues. (H). Percent of tunel$^+$ cells in each group. $n = 10$ mice/group. A minimum of three independent experiments were performed. $^{\#\#}P < 0.01$, $^{\#\#\#}P < 0.001$ compared to control; $^{*}P < 0.05$, $^{**}P < 0.01$ compared to IR group. CNC: *Camellia nitidissima* Chi; H&E: Hematoxylin and eosin; IR: Irradiated; TAI: Total abdominal irradiation.

analysis indicated that the anal canals of mice in the irradiated group had obvious fouling with bloody stools, indicating that radiation severely disrupted intestinal homeostasis and caused abnormal feces. Although the CNC-treated mice had diarrhea symptoms, no bloody stools were observed, indicating that CNC alleviated

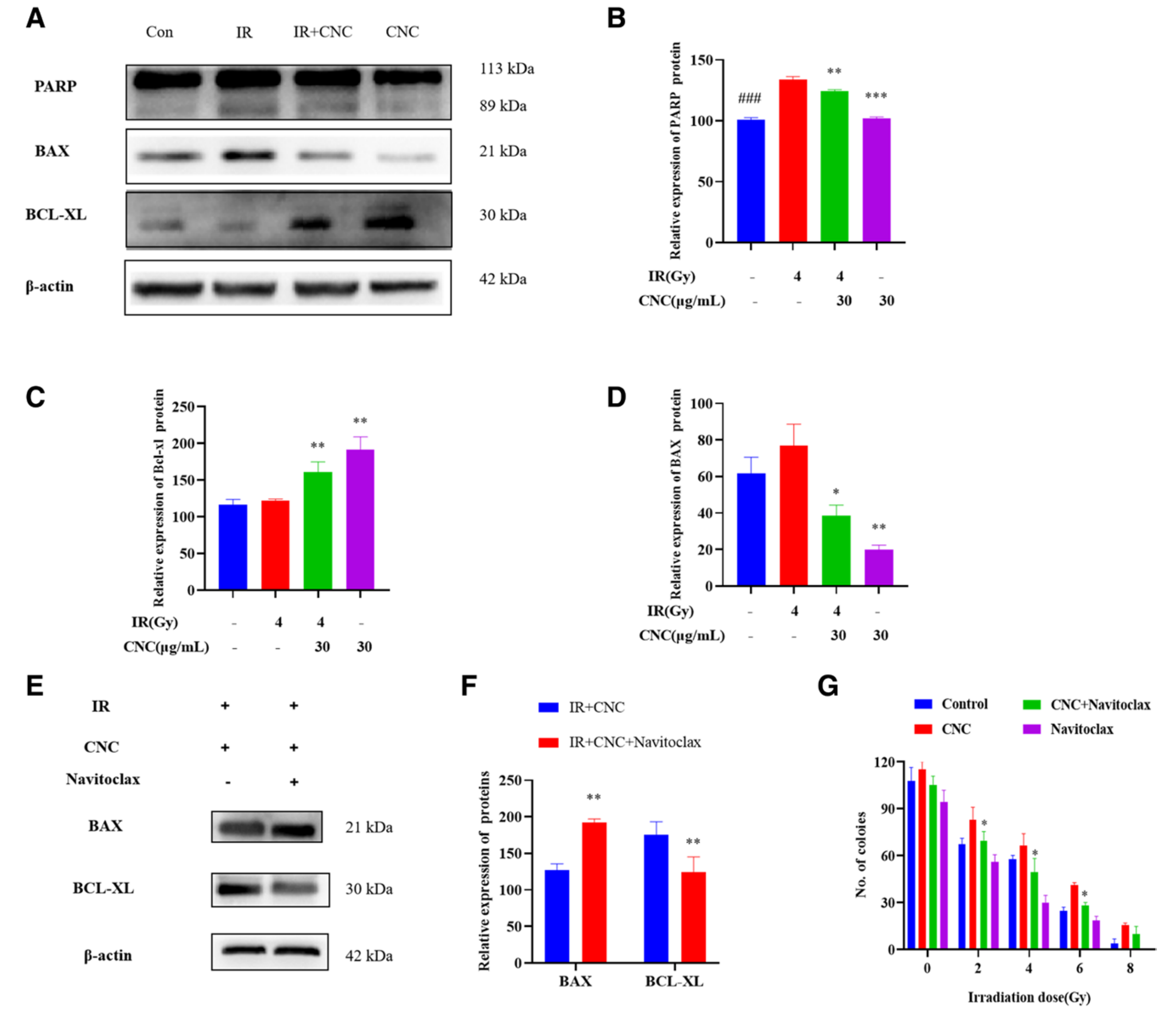

Figure 8. CNC can inhibit radiation-induced cell death. (A). Effect of CNC on regulatory protein expression. Quantitative analysis of proteins associated with loss of regulation in (B), (C), and (D). (E). The addition of the BCL-2 inhibitor, navitoclax, resulted in changes in the expression of BAX and BCL-XL. (F). Quantitative analysis of BAX and BCL-XL protein expression (G). Changes in colony formation in HIEC-6 cells were observed after navitoclax addition. Data are expressed as the mean ± SD of three independent experiments (n = 3). A minimum of three independent experiments were performed. $^{###}P < 0.001$ compared with control; $^{*}P < 0.05$, $^{**}P < 0.01$, compared with the IR group. BAX: Bcl-2–associated X protein; BCL-XL: B-cell lymphoma-extra large; CNC: *Camellia nitidissima* Chi; IR: Irradiated; PARP: Poly ADP-ribose polymerase; SD: Standard deviation.

the gastrointestinal damage caused by irradiation to some extent.

After assessing the impact of CNCs on cell viability, we discovered that CNCs increased cell viability without affecting HIEC-6 cells exposed for 24, 48, and 72 h. Subsequently, the colony formation experiment results demonstrated that CNC could effectively promote HIEC-6 cell proliferation compared to those in the untreated control and irradiated groups, indicating that CNC may exert a radioprotective effect by promoting cell proliferation. Using western blotting, we found that CNC increased the expression of BCL-XL[55] and inhibited the expression of BAX[56] and PARP[55,57,58]. At the same time, we selected Navitoclax, a BCL-2 inhibitor, to verify the inhibitory effect of CNC on BAX. These results further verify the previous experimental results and prove that CNC exerts radiation-protective effects by inhibiting apoptosis (Figure 9).

Conclusions

CNC has a strong antioxidant ability, can improve the survival rate of mice under lethal dose irradiation, and plays a protective role against radiation-induced damage to the hematopoietic and gastrointestinal systems. Overall, this Chinese herbal medicine has significant potential as a protective agent against radiation damage and warrants further in-depth studies.

Conflict of interest statement

The authors declare no conflict of interest.

Funding

This work was sponsored by the National Natural Science Foundation of China (82303681 and 82202950), Fundamental Research Funds for the

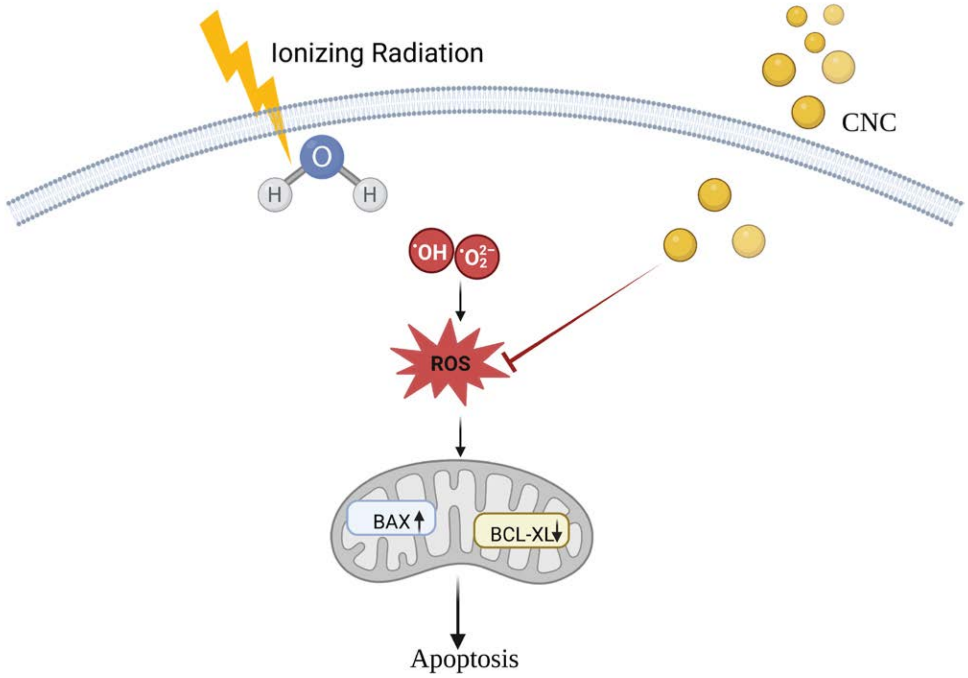

Figure 9. Schematic showing the radioprotective role of CNC. CNC regulates ROS-induced apoptosis and plays a radioprotective role. BAX: Bcl-2–associated X protein; BCL-XL: B-cell lymphoma-extra large; CNC: *Camellia nitidissima* Chi; ROS: Reactive oxygen species.

Central Universities (3332022063), and the Chinese Academy of Medical Sciences Innovation Fund for Medical Sciences (2021-I2M-1-042). The National Natural Science Foundation of China (82202950) and the Fundamental Research Funds for the Central Universities (3332022063) were held by Feifei Xu, who participated in the research design. The National Natural Science Foundation of China (82303681) was held by Wenfeng Gou, who participated in the research design. The Chinese Academy of Medical Sciences Innovation Fund for Medical Sciences (2021-I2M-1-042) was held by Wenbin Hou, who designed and conceived the study.

Author contributions

Zhiyun Wang and Haihua Shang designed and conceived the study, performed relevant analyses, and drafted the manuscript. Wenfeng Gou and Feifei Xu participated in the research design. Yue Hou, Gaiting Liu, Zhonghao Ren, Yuhua Tian, and Yiliang Li acquired and analyzed the data. Wei Li, Yuefei Wang, and Wenbin Hou designed and conceived the study. All the authors have read and approved the final version of the manuscript.

Ethical approval of studies and informed consent

This study was reviewed and approved by the Animal Ethics Committee of the Institute of Radiation Medicine, Chinese Academy of Medical Sciences, under the ethics number: IRM-DWLL-20211218, IRMDWLL-20211219, IRM-DWLL-20211220.

Acknowledgments

None.

Data availability

All data generated or analyzed during this study are included in this published article (and its SDC files).

References

[1] Schaich KM, Pryor WA. Free radical initiation in proteins and amino acids by ionizing and ultraviolet radiations and lipid oxidation—part III: free radical transfer from oxidizing lipids. *Crit Rev Food Sci Nutr* 1980;13(3):189–244.
[2] Chambers CE. Health risks of ionizing radiation: Dr Roentgen today. *Circulation* 2017;136(25):2417–2419.
[3] Einor D, Bonisoli-Alquati A, Costantini D, et al. Ionizing radiation, antioxidant response and oxidative damage: a meta-analysis. *Sci Total Environ* 2016;548-549:463–471.
[4] Yang P, Luo X, Li J, et al. Ionizing radiation upregulates glutamine metabolism and induces cell death via accumulation of reactive oxygen species. *Oxid Med Cell Longev* 2021;2021:5826932.
[5] Haimovitz-Friedman A, Kan CC, Ehleiter D, et al. Ionizing radiation acts on cellular membranes to generate ceramide and initiate apoptosis. *J Exp Med* 1994;180(2):525–535.
[6] Wei Y, Gong Y, Wei S, et al. Protection of the hematopoietic system against radiation-induced damage: drugs, mechanisms, and developments. *Arch Pharm Res* 2022;45(8):558–571.
[7] Yu X, Li M, Zhu L, et al. Amifostine-loaded armored dissolving microneedles for long-term prevention of ionizing radiation-induced injury. *Acta Biomater* 2020;112:87–100.
[8] Khan S, Adhikari JS, Rizvi MA, et al. Melatonin attenuates ^{60}Co γ-ray-induced hematopoietic, immunological and gastrointestinal injuries in C57BL/6 male mice. *Environ Toxicol* 2017;32(2):501–518.
[9] Wang Y, Liu L, Pazhanisamy SK, et al. Total body irradiation causes residual bone marrow injury by induction of persistent oxidative stress in murine hematopoietic stem cells. *Free Radic Biol Med* 2010;48(2):348–356.
[10] Spencer CM, Goa KL. Amifostine. A review of its pharmacodynamic and pharmacokinetic properties, and therapeutic potential as a radioprotector and cytotoxic chemoprotector. *Drugs* 1995;50(6):1001–1031.
[11] Mahady GB. Global harmonization of herbal health claims. *J Nutr* 2001;131(3s):1120S–1123S.
[12] Jang H, Lee J, Park S, et al. Baicalein mitigates radiation-induced enteritis by improving endothelial dysfunction. *Front Pharmacol* 2019;10:892.

[13] Gao J, Peng S, Shan X, et al. Inhibition of AIM2 inflammasome-mediated pyroptosis by andrographolide contributes to amelioration of radiation-induced lung inflammation and fibrosis. *Cell Death Dis* 2019;10(12):957.

[14] Li X, Yi J, Zhu J, et al. Protective effect of coix seed seedling extract on ^{60}Co-γ radiation-induced oxidative stress in mice. *J Food Sci* 2022;87(1):438–449.

[15] Xie LW, Cai S, Zhao TS, et al. Green tea derivative (-)-epigallocatechin-3-gallate (EGCG) confers protection against ionizing radiation-induced intestinal epithelial cell death both *in vitro* and *in vivo*. *Free Radic Biol Med* 2020;161:175–186.

[16] Wu X, He FL, Pan HF, et al. Characterization of the plastome of Camellia pingguoensis (Theaceae), an endangered and endemic yellow camellia species in China. *Mitochondrial DNA B Resour* 2020;5(3):3527–3528.

[17] Zhang X, Feng J, Su S, et al. Hepatoprotective effects of Camellia nitidissima aqueous ethanol extract against CCl4-induced acute liver injury in SD rats related to Nrf2 and NF-κB signalling. *Pharm Biol* 2020;58(1):239–246.

[18] Hou X, Du H, Yang R, et al. The antitumor activity screening of chemical constituents from Camellia nitidissima Chi. *Int J Mol Med* 2018;41(5):2793–2801.

[19] He X, Li H, Zhan M, et al. Camellia nitidissima Chi extract potentiates the sensitivity of gastric cancer cells to paclitaxel via the induction of autophagy and apoptosis. *Onco Targets Ther* 2019;12:10811–10825.

[20] Yang R, Guan Y, Wang W, et al. Antioxidant capacity of phenolics in Camellia nitidissima Chi flowers and their identification by HPLC Triple TOF MS/MS. *PLoS One* 2018;13(4):e0195508.

[21] Zhang HL, Wu QX, Qin XM. Camellia nitidissima Chi flower extract alleviates obesity and related complications and modulates gut microbiota composition in rats with high-fat-diet-induced obesity. *J Sci Food Agric* 2020;100(12):4378–4389.

[22] Yang R, Guan Y, Zhou J, et al. Phytochemicals from Camellia nitidissima Chi flowers reduce the pyocyanin production and motility of Pseudomonas aeruginosa PAO1. *Front Microbiol* 2018;8:2640.

[23] Chen Y, Hao E, Zhang F, et al. Identifying active compounds and mechanism of Camellia nitidissima Chi on anti-colon cancer by network pharmacology and experimental validation. *Evid Based Complement Alternat Med* 2021;2021:7169211.

[24] Waselenko JK, MacVittie TJ, Blakely WF, et al. Medical management of the acute radiation syndrome: recommendations of the Strategic National Stockpile Radiation Working Group. *Ann Intern Med* 2004;140(12):1037–1051.

[25] Wang K, Tepper JE. Radiation therapy-associated toxicity: etiology, management, and prevention. *CA Cancer J Clin* 2021;71(5):437–454.

[26] Wu S, Chang H, Gou W, et al. Protective effects of Engelhardia roxburghiana Wall. leaf extract on radiation injury of the hematopoietic system in mice. *Int J Radiat Med Nucl Med* 2022;46(2):92–102.

[27] Wu S, Tian C, Tu Z, et al. Protective effect of total flavonoids of Engelhardia roxburghiana Wall. leaves against radiation-induced intestinal injury in mice and its mechanism. *J Ethnopharmacol* 2023;311(311):116428.

[28] Picard C, Ksas B, Griffiths NM, et al. Effect of granisetron on radiation-induced alterations of colonic motility and fluid absorption in rats. *Aliment Pharmacol Ther* 2002;16(3):623–631.

[29] Azzam EI, De Toledo SM, Little JB. Oxidative metabolism, gap junctions and the ionizing radiation-induced bystander effect. *Oncogene* 2003;22(45):7050–7057.

[30] Hu L, Yin X, Zhang Y, et al. Radiation-induced bystander effects impair transplanted human hematopoietic stem cells via oxidative DNA damage. *Blood* 2021;137(24):3339–3350.

[31] Ma JS, Liu H, Han CR, et al. Extraction, characterization and antioxidant activity of polysaccharide from Pouteria campechiana seed. *Carbohydr Polym* 2020;229:115409.

[32] Dong H, Lin S, Zhang Q, et al. Effect of extraction methods on the properties and antioxidant activities of Chuanminshen violaceum polysaccharides. *Int J Biol Macromol* 2016;93(Pt A):179–185.

[33] Rai Y, Pathak R, Kumari N, et al. Mitochondrial biogenesis and metabolic hyperactivation limits the application of MTT assay in the estimation of radiation induced growth inhibition. *Sci Rep* 2018;8(1):1531.

[34] Crowe ME, Lieven CJ, Thompson AF, et al. Borane-protected phosphines are redox-active radioprotective agents for endothelial cells. *Redox Biol* 2015;6:73–79.

[35] Singh VK, Seed TM. Entolimod as a radiation countermeasure for acute radiation syndrome. *Drug Discov Today* 2021;26(1):17–30.

[36] Hérodin F, Bourin P, Mayol JF, et al. Short-term injection of antiapoptotic cytokine combinations soon after lethal gamma-irradiation promotes survival. *Blood* 2003;101(7):2609–2616.

[37] Anno GH, Young RW, Bloom RM, et al. Dose response relationships for acute ionizing-radiation lethality. *Health Phys* 2003;84(5):565–575.

[38] Zhang S, Dong J, Li Y, et al. Gamma-irradiation fluctuates the mRNA N6-methyladenosine (m^6A) spectrum of bone marrow in hematopoietic injury. *Environ Pollut* 2021;285:117509.

[39] Hardmeier R, Hoeger H, Fang-Kircher S, et al. Transcription and activity of antioxidant enzymes after ionizing irradiation in radiation-resistant and radiation-sensitive mice. *Proc Natl Acad Sci U S A* 1997;94(14):7572–7576.

[40] Bump EA, Brown JM. Role of glutathione in the radiation response of mammalian cells *in vitro* and *in vivo*. *Pharmacol Ther* 1990;47(1):117–136.

[41] Obrador E, Salvador R, Villaescusa JI, et al. Radioprotection and radiomitigation: from the bench to clinical practice. *Biomedicines* 2020;8(11):461.

[42] Stenke L, Lindberg K, Lagergren Lindberg M, et al. Coordination of management of the acute radiation syndrome. *Radiat Prot Dosimetry* 2018;182(1):80–84.

[43] Das U, Sengupta A, Biswas S, et al. Alteration of murine duodenal morphology and redox signalling events by reactive oxygen species generated after whole body γ-irradiation and its prevention by ferulic acid. *Free Radic Res* 2017;51(11-12):886–910.

[44] Zhang LY, Zhou T, Zhang YM, et al. Guiqi Baizhu Decoction alleviates radiation inflammation in rats by modulating the composition of the gut microbiota. *Evid Based Complement Alternat Med* 2020;2020:9017854.

[45] Metcalfe C, Kljavin NM, Ybarra R, et al. Lgr5+ stem cells are indispensable for radiation-induced intestinal regeneration. *Cell Stem Cell* 2014;14(2):149–159.

[46] Fliedner TM, Graessle D, Meineke V, et al. Pathophysiological principles underlying the blood cell concentration responses used to assess the severity of effect after accidental whole-body radiation exposure: an essential basis for an evidence-based clinical triage. *Exp Hematol* 2007;35(4 Suppl 1):S8–S16.

[47] MacNaughton WK. Therapeutics. Review article: new insights into the pathogenesis of radiation-induced intestinal dysfunction. *Aliment Pharmacol Ther* 2000;14(5):523–528.

[48] Meistrich ML, Kangasniemi M. Hormone treatment after irradiation stimulates recovery of rat spermatogenesis from surviving spermatogonia. *J Androl* 1997;18(1):80–87.

[49] Pena LA, Fuks Z, Kolesnick RN. Radiation-induced apoptosis of endothelial cells in the murine central nervous system: protection by fibroblast growth factor and sphingomyelinase deficiency. *Cancer Res* 2000;60(2):321–327.

[50] Geiger H, Pawar SA, Kerschen EJ, et al. Pharmacological targeting of the thrombomodulin-activated protein C pathway mitigates radiation toxicity. *Nat Med* 2012;18(7):1123–1129.

[51] Kiang JG, Olabisi AO. Bioscience. Radiation: a poly-traumatic hit leading to multi-organ injury. *Cell Biosci* 2019;9(1):1–15.

[52] Seed TM. Radiation protectants: current status and future prospects. *Health Phys* 2005;89(5):531.

[53] Dubois A, Walker RI. Prospects for management of gastrointestinal injury associated with the acute radiation syndrome—ScienceDirect. *Gastroenterology* 1988;95(2):500–507.

[54] Kong P, Yang M, Wang Y, et al. Ferroptosis triggered by STAT1-IRF1-ACSL4 pathway was involved in radiation-induced intestinal injury. *Redox Biol* 2023;66:102857.

[55] Bharti V, Watkins R, Kumar A, et al. BCL-xL inhibition potentiates cancer therapies by redirecting the outcome of p53 activation from senescence to apoptosis. *Cell Rep* 2022;41(12):111826.

[56] Men J, Zhang L, Peng R, et al. Metformin ameliorates 2.856 GHz microwave- radiation-induced reproductive impairments in male rats via inhibition of oxidative stress and apoptosis. *Int J Mol Sci* 2023;24(15):12250.

[57] Li WH, Wang F, Song GY, et al. PARP-1: a critical regulator in radioprotection and radiotherapy-mechanisms, challenges, and therapeutic opportunities. *Front Pharmacol* 2023;14:1198948.

[58] El-Sheikh MM, Abdel-Naby DH, El-Hazek RM, et al. Regulation of radiation-induced liver damage by modulation of SIRT-1 activity: *in vivo* rat model. *Cell Biochem Funct* 2023;41(1):67–77.